2015 IEEE/RSJ International Conference on Intelligent Robots and Systems (IROS)
Congress Center Hamburg
Sept 28 - Oct 2, 2015. Hamburg, Germany

A New Passivity-Based Control Technique for Safe Patient-Robot Interaction in Haptics-Enabled Rehabilitation Systems*

S. Farokh Atashzar, Mahya Shahbazi, Mahdi Tavakoli, Rajni V. Patel

***Abstract*— In this paper, a new passivity-based technique is proposed to analyze and guarantee the stability of haptics-enabled telerobotic rehabilitation systems where there is a possibility of having more sources of non-passivity than communication delays. In practice, the difficulty of therapeutic exercises should be tuned taking into account the stage of physical disability. However, tuning the difficulty and intensity should not violate the stability of patient-robot interaction. This usually puts conservative prefixed limits on the allowable exercise intensity. In this paper, patient-robot interaction safety is studied in the context of Strong Passivity Theory (SPT). Our goal is to ultimately relax the limitation on the allowable robotic therapies while preserving system stability. The proposed stabilizing scheme does not try to make the entire non-passive component passive. This allows the therapist to have freedom in injecting energy into the system for assistive therapies while ensuring safe patient-robot interaction. In this paper, the case of telerobotic rehabilitation is considered. Experimental implementation and evaluation are presented to support the proposed theory.**

I. Introduction

There are two types of therapeutic procedures that can be delivered by Haptics-enabled Robotic Rehabilitation (HRR) systems: (a) Assistive Therapy (AT), mostly administered in early stages of rehabilitation, and (b) Resistive Therapy (RT), mostly considered for later stages of therapy. During assistive therapy, the haptic device helps the patient to perform movements for accomplishing tasks, while during resistive therapy the haptic device resists the movements initiated by the patient [1], [2]. Conventional HRR systems are composed of three major components: (a) a powerful haptic device that registers the patient's motion profiles and applies assistive/resistive forces, (b) a game-like virtual reality (VR) to provide visual cues, and (c) Programmable Virtual Therapist (PVT) software that uses the measured data and determines the extent of therapy to be delivered [1], [2], [3]. A representative HRR system is shown in Fig. 1.

* This research was supported by the Canadian Institutes of Health Research (CIHR) and the Natural Sciences and Engineering Research Council (NSERC) of Canada under the Collaborative Health Research Projects (CHRP) Grant #316170; an NSERC Collaborative Research and Development Grant # CRDPJ 411603-10 with industrial partner, Quanser Inc.; the AGE-WELL Network of Centres of Excellence under the project AW CRP 2015-WP5.3; the Canada Foundation for Innovation (CFI) under grant LOF 28241; and the Alberta Innovation and Advanced Education Ministry under Small Equipment Grant RCP-12-021. S.F. Atashzar, M. Shahbazi, and R.V. Patel are with Canadian Surgical Technologies and Advanced Robotics (CSTAR), and with the Department of Electrical and Computer Engineering, Western University, London, ON, Canada (email: satashza@uwo.ca, mshahba2@uwo.ca, rvpatel@uwo.ca). R.V. Patel is also with the Department of Surgery at Western University. M. Tavakoli is with the Department of Electrical and Computer Engineering, University of Alberta, Edmonton, AB, Canada (email: mahdi.tavakoli@ualberta.ca).

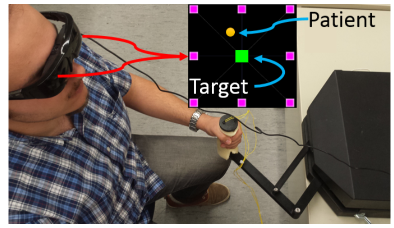

Fig. 1. A haptics-enabled robotic rehabilitation system.

Research has shown that the key to an effective therapy is to modify the difficulty level of exercises, considering the state and progress of the patient [4]. There are some adaptive techniques proposed in the literature to tune features of robotic therapy based on sensorimotor measurements. However, the direct contribution of a skilled human therapist in the interactive process of rehabilitation is bypassed using PVT-based systems, which limits the ability of the therapist in choosing the best position/force trajectories and tasks for rehabilitation and assessment. To address this issue, the authors have recently analyzed the feasibility of a Haptics-enabled Telerobotic Rehabilitation (HTR) architecture that can combine the advantages of conventional HRR systems and the skills of a human therapist in the rehabilitation loop to provide patients with an augmented therapeutic environment [5], [6] . The proposed HTR system can be combined with artificial intelligence algorithms to allow therapists to program and calibrate HRR systems regarding the required difficulty and strategy of the therapy (this is part of ongoing research of our team e.g. [7]). Telerobotic rehabilitation also enables remote and in-home assessment and therapy, which is a need for patients in areas far from sophisticated rehabilitation centres [8]. Although there are advantages to the use of robotic and telerobotic technologies for in-place and remote assessment and rehabilitation, the safety of patient-robot interactions remains a concern, especially when high control effort is needed and/or when the robot is to be used remotely in a patient's home. This can limit the allowable therapy intensity, and puts conservative caps on the administered forces [9] and reduces the effectiveness.

In this paper, a new control architecture is proposed in the context of strong passivity theory (SPT) for haptic systems. The technique quantifies the Shortage of Passivity (SOP) of the delivered therapy and the EOP of the patient's, and uses these measures to find an patient-specific tuning strategy that modifies the therapeutic energy, to guarantee system stability and patient safety. Experimentally evaluation is given on an implementation of the HTR architecture, shown in Fig. 2.

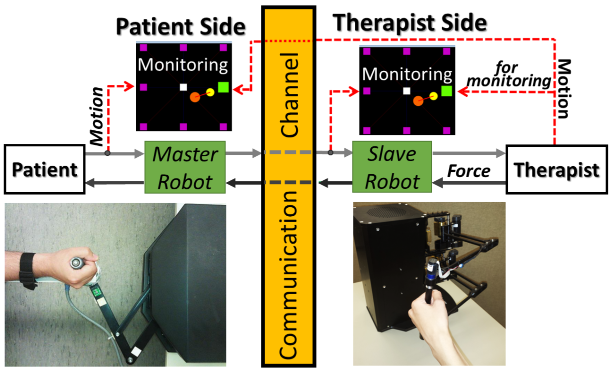

Fig. 2. A schematic of the implemented HTR system used in this paper. The shared virtual environment (the square with black background) is monitored for both the therapist and the patient, where the assigned target location, home-position, and motions of the patient (shown by the orange circle) and the therapist (shown by the yellow circle) can be observed. The communication channel can be home-hospital and/or clinic-clinic networks.

II. System Modeling and Transparency Analysis

A transparent 2-channel bilateral model [10] is considered for HTR systems as a modification of the extended Lawrence four-channel architecture [11], [12]. The patient handles the master robot which allows them to apply different motion trajectories. The therapist interacts with the slave robot, so he/she can feel the patient's motions and provide forces in response, to deliver the needed resistive/assistive therapy.

A. Local Interaction Modeling

The linearized dynamics of the Patient-Robot (P-R) interaction can be written as

$$z_m(t) * v_p(t) = u_{cm}(t) + f_p(t). \qquad (1)$$

In (1), t is time, $*$ is the convolution operator, $z_m(t)$ is the impulse response of the linearized master robot dynamics, $u_{cm}(t)$ is the control input for the master device delivering the needed therapy, $v_p(t)$ is the patient's hand velocity, and $f_p(t)$ is the force applied by the patient and can be decomposed into "active"and "reactive" components as

$$f_p(t) = f_p^*(t) - f_{react}(t), \quad \text{where} \quad f_{react} = z_p(v_p, t) \qquad (2)$$

In (2), $z_p(v_p, t)$ is a non-autonomous nonlinear impedance model for the mechanical reaction of the patient's hand in response to the master robot movements. Also, $f_p^*(t)$ is the voluntary component applied by the musculoskeletal system of the patient's arm to generate motions.

The dynamics of the Therapist-Robot (T-R) interaction are

$$z_s(t) * v_{th}(t) = u_{cs}(t) + f_{th}(t) \qquad (3)$$

where $z_s(t)$ is the impulse response of the linearized slave dynamics, $u_{cs}(t)$ is the control input for the slave device, $v_{th}(t)$ is the therapist's hand velocity, and $f_{th}(t)$ is the force applied by the therapist to administer an appropriate therapy. The therapist's force decomposition can be achieved as

$$f_{th}(t) = f_{th}^*(t) - z_{th}(v_{th}, t) \qquad (4)$$

This means that the therapist can provide various therapeutic forces through exogenous component f_{th}^* and her/his hand's

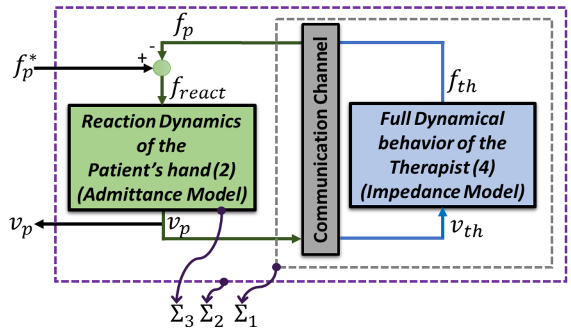

Fig. 3. The overall schematic of the designed interconnection. The subsystem Σ_1 is called the "therapy terminal". Σ_1 consists of the communication and any behavior of the therapist. Also, the system defined by Σ_2 is the entire interaction, which gets f_p^* as the input and provides v_p as the output. Σ_3 is the admittance model of the patient's hand mechanical reaction.

nonlinear impedance model $z_{th}(v_{th}, t)$. In this paper We assume that the therapist does not change z_{th} frequently. This assumption will be relaxed in the future work of this paper.

B. Transparency Analysis

In order to provide the patient with high fidelity administered therapy and the therapist with an accurate feel of the patient's hand movement trajectory, a transparent two-channel teleoperation architecture (which was proposed by the authors in [10]) is considered. The utilized architecture is a new modification of the conventional extended Lawrence four-channel scheme [11] that uses the minimum number of communication channels (two) while guaranteeing system transparency (fidelity). To implement the architecture, the control signals $u_{cm}(t)$ and $u_{cs}(t)$ should be calculated based on (5) for the master robot and (6) for the slave robot:

$$u_{cm}(t) = c_1(t) * v_p(t) - \hat{f}_{th}(t) \quad where \quad c_1(t) = z_m(t) \qquad (5)$$

$$u_{cs}(t) = -f_{th}(t) + c_2(t) * \hat{v}_p(t) \quad where \quad c_2(t) = z_s(t) \qquad (6)$$

In (5) and (6), $\hat{f}_{th}(s)$ is the received therapeutic force at the patient-side, sent through the first communication channel, and $\hat{v}_p(t)$ is the received patient's hand velocity at the therapist-side, sent through the second communication channel. In order to consider the case of remote rehabilitation, the communication is assumed to involve a time-varying time delay defined by $\tau(t)$. Consequently we have: $\hat{f}_{th}(t) = f_{th}(t - \tau(t))$, and $\hat{v}_p(t) = v_p(t - \tau(t))$. Combining the control signals defined in (5) and (6) with (1) and (3), the transparency of the patient-therapist interaction is guaranteed, as shown below:

$$\begin{aligned} f_p(t) &= \hat{f}_{th}(t), \\ v_{th}(t) &= \hat{v}_p(t). \end{aligned} \qquad (7)$$

The resulting 2-channel interconnection between the patient's admittance and the therapist's impedance is given in Fig. 3.

III. The Excess of Passivity Analysis

Although the resistive therapy is a passive action, assistive therapy is non-passive since the therapist needs to inject energy into the system to amplify/coordinate the patient's efforts [13]. In addition, for the remote rehabilitation scenario, the communication delay adds further to the non-passivity. Here, a one-port "Therapy Terminal" is defined

(Σ_1 in Fig. 3) by combining the aforementioned sources of non-passive behavior. In order to study the stability of the entire system, the following hypothesis is proposed.

Hypothesis I. *When there is a non-passive therapy terminal (Σ_1) in a haptics-enabled rehabilitation system, the closed-loop interaction can still remain stable if the passivity of the patient's hand can compensate for the shortage of passivity at the therapy terminal Σ_1.*

The remainder of this section focuses on how this hypothesis can be mathematically proved.

Remark I. In the conventional usage of passivity theory [14], [15], assuming a passive operator and environment terminations for a telerobotic system, the communication channel passivity provides a negative interconnection of serial passive subsystems, which remains stable. This is called the Weak Passivity Theorem, which is widely used in conventional telerobotic systems to design various controllers to passify the communication channel in isolation to keep the entire system passive [16]. However, for rehabilitation systems, since the one-port therapy terminal Σ_1 can be non-passive, the entire interaction Σ_2 can be non-passive even if the communication channel is passive (i.e., no delay). It is counterproductive to directly passify the non-passive therapist since it defeats the very purpose of assistance to damp all the injected therapeutic energy. Consequently, to preserve interaction safety while still letting the non-passive therapy terminal Σ_1 inject energy, the passivity of the whole interconnection Σ_2 should be analyzed instead of passivity of isolated components. This has correlations with the definition of the Strong Passivity Theory given in [15], [17].

For this goal and to validate Hypothesis I, first the mathematical definitions of a Passive Model, Input-Passive Model, and Output-Passive Model for a system with input vector $u_{in}(t)$, output vector $y_{out}(t)$, and initial energy β at $t = 0$ are given [15], [18], [19].

Definition I. *If there exists a constant β such that for all $t \geq 0$ we have*

$$\int_0^t u_{in}(\tau)^T \cdot y_{out}(\tau)\, d\tau \geq \beta, \tag{8}$$

the system is passive.

Definition II. *If there exists a constant β such that for all $t \geq 0$ we have*

$$\int_0^t u_{in}(\tau)^T \cdot y_{out}(\tau)\, d\tau \geq \beta + \delta \cdot \int_0^t u_{in}(\tau)^T \cdot u_{in}(\tau)\, d\tau, \tag{9}$$

for $\delta \geq 0$, the system is Input Strictly Passive (ISP) and the corresponding excess of passivity (EOP) is equal to δ. Also, if we have $\delta < 0$, the system is Input Nonpassive (INP) and the Shortage of Passivity (SOP) of the system is δ.

Definition III. *If there exists a constant β such that for all $t \geq 0$ we have*

$$\int_0^t u_{in}(\tau)^T \cdot y_{out}(\tau)\, d\tau \geq \beta + \xi \cdot \int_0^t y_{out}(\tau)^T \cdot y_{out}(\tau)\, d\tau, \tag{10}$$

for $\xi \geq 0$, the system is Output Strictly Passive (OSP) and the EOP is ξ. Also if we have $\xi < 0$, the system is Output Nonpassive (ONP) and the SOP is ξ.

Remark II. It has been shown that a passive system is asymptotically stable and an output strictly passive system is L_2 stable [20]. For the case of L_2 stability, the finite L_2 gain of the system is less than or equal to $1/\xi$ where ξ is the EOP of the OSP system. The definition of L_2 stability is given below ($\alpha_0 \geq 0$ is a function of the initial energy):

$$\|y_o(t)\|_{L_2} \leq 1/\xi \cdot \|u_i(t)\|_{L_2} + \alpha_0 \tag{11}$$

In order to validate Hypothesis I, consider the entire system as the one-port network Σ_2 shown in Fig. 3. Σ_2 consists of a non-passive therapy-terminal impedance Σ_1 and a passive reaction admittance Σ_3. The exogenous force $f_p^*(t)$ is the external input and the velocity of the patient's hand $v_p(t)$ is the response to this input. Consequently, in order to guarantee stability, the following passivity condition should be checked assuming zero initial condition:

$$\int_0^t f_p^*(\tau)^T \cdot v_p(\tau)\, d\tau \geq 0, \tag{12}$$

Considering (12) and (2) we have

$$\begin{aligned} &\int_0^t f_p^*(\tau)^T \cdot v_p(\tau)\, d\tau = \\ &\int_0^t f_p(\tau)^T \cdot v_p(\tau)\, d\tau + \int_0^t f_{react}(\tau)^T \cdot v_p(\tau)\, d\tau. \end{aligned} \tag{13}$$

As a result, the passivity condition for Σ_2 is achieved as

$$\int_0^t f_p(\tau)^T \cdot v_p(\tau)\, d\tau + \int_0^t f_{react}(\tau)^T \cdot v_p(\tau)\, d\tau \geq 0. \tag{14}$$

It can be seen from Fig. 3 that $\int_0^t f_{react}(\tau)^T \cdot v_p(\tau)\, d\tau$ is the passivity integral of the patient hand's reaction dynamics Σ_3 and $\int_0^t f_p(\tau)^T \cdot v_p(\tau)\, d\tau$ is that of the therapy terminal Σ_1. Consequently, considering the passivity condition (14), if the therapy terminal Σ_1 behaves as a non-passive system, the entire system can still remain passive if the energy of the reaction dynamics of the patient's hand, i.e. $\int_0^t f_{react}(\tau)^T \cdot v_p(\tau)\, d\tau$, can compensate for the injected energy by the therapist terminal. Considering the passivity condition (14) and the definition of L_2 stability given in Remark II when initial energy at $t = 0$ is zero, we have that:

$$\begin{aligned} &\text{the system } \Sigma_2 \text{ is } L_2 \text{ stable if } \exists\ \xi_r > 0 \text{ s.t.} \\ &\int_0^t f_p(\tau)^T \cdot v_p(\tau)\, d\tau + \int_0^t f_{react}(\tau)^T \cdot v_p(\tau)\, d\tau \\ &\qquad \geq \xi_r \cdot \int_0^t v_P(\tau)^T \cdot v_p(\tau)\, d\tau. \end{aligned} \tag{15}$$

Considering an INP model for Σ_1 with shortage of passivity $\hat{\delta}_{th} \leq 0$, and an OSP model for the patient reaction admittance Σ_3 with excess of passivity $\xi_p \geq 0$, for Σ_1 and Σ_3 we have:

$$\begin{aligned} \int_0^t f_p(\tau)^T \cdot v_p(\tau)\, d\tau \geq \hat{\delta}_{th} \cdot \int_0^t v_P(\tau)^T \cdot v_p(\tau)\, d\tau, \\ \text{s.t. } \hat{\delta}_{th} \leq 0 \end{aligned} \tag{16}$$

$$\begin{aligned} \int_0^t f_{react}(\tau)^T \cdot v_p(\tau)\, d\tau \geq \xi_p \cdot \int_0^t v_P(\tau)^T \cdot v_p(\tau)\, d\tau, \\ \text{s.t. } \xi_p \geq 0 \end{aligned} \tag{17}$$

Combining (15), (16), and (17) we have that:

$$\text{the interconnection is } L_2 \text{ stable if} \quad (\xi_p+\hat{\delta}_{th}-\xi_r)\cdot\int_0^t v_P(\tau)^T\cdot v_p(\tau)\,d\tau \geq 0 \quad (18)$$

Considering (18) and also a small positive arbitrary value ξ_r, the new stability condition can be calculated as given below:

$$\xi_p+\hat{\delta}_{th}-\xi_r \geq 0 \quad (19)$$

In (19), ξ_r defines a stability margin. As a result, the entire system will remain L_2 stable, considering the stability margin ξ_r, if the EOP of the reaction dynamics of the patient's hand (δ_p) can compensate for the SOP of the therapy terminal (in other words, δ_p should provide a minimum level of excess of passivity $\delta_p > |\xi_r|+|\hat{\delta}_{th}|$). This validates Hypothesis I, and provides a new stability analysis for haptics-enabled systems.

IV. Proposed EOP/SOP Estimator and Controller

The purpose of this section is to develop a stabilizing scheme, based on the stability conditions (19), to modify the administered therapy, guarantee stability and allow the therapist to inject energy into the interconnection during assistance. The proposed controller has three components: (a) stabilizer, (b) EOP estimator for the reaction dynamics of patient's hand, (c) SOP observer for the therapy terminal.

A. Stabilizer

As mentioned earlier, a straightforward technique to guarantee interaction passivity is to dampen out the entire non-passive energy injected by the therapy terminal. However, this will result in significantly undermining the assistive therapy. To design a less-conservative scheme, a damping (i.e. η) is implemented on the patient's side, in parallel to Σ_1, based on the following therapist force modification law:

$$\hat{f}_{th-mod}(t) = \hat{f}_{th}(t)+\eta_c\cdot v_p(t). \quad (20)$$

In (20), $\hat{f}_{th-mod}$ is the modification of the therapeutic force ($\hat{f}_{th}$) which will be reflected to the patient's hand to stabilize the system. Based on the transparency features of the utilized two-channel architecture, given in (7), and considering the modified reflected force (shown in (20)), we have:

$$f_p(t) = \hat{f}_{th}(t)+\eta_c\cdot v_p(t). \quad (21)$$

Combining (21), (15), the new L_2 stability condition, including the proposed stabilizing damper (η_c), will be

$$\int_0^t (\xi_p+\hat{\delta}_{th}-\xi_r+\eta_c(t))\cdot v_P(\tau)^T\cdot v_p(\tau)\,d\tau \geq 0 \quad (22)$$

As a result, the new stabilizing condition for the proposed rehabilitation architecture is achieved, as given below:

$$\eta(t) \geq \xi_r-\psi, \quad \text{where } \psi = \xi_p+\hat{\delta}_{th} \quad (23)$$

In (23), ψ is the numeric value showing the "deviation level" from the stability criterion and ξ_r is an arbitrary positive value that provides a safety margin to address uncertainties.

Based on (23), the required damping factor, $\eta_{min}(t)$, which should be injected to guarantee L_2 stability while allowing the therapist to assist the patient, can be calculated as

$$\eta_{min}(t) = 0.5(1+Sign(\xi_r-\psi))\cdot(\xi_r-\psi) \quad (24)$$

Considering (24), if deviation from the calculated stability condition is zero, the controller does not inject damping into the interconnection, while if the amplitude of the SOP of the prescribed therapy ($\hat{\delta}_{th}$) is higher than the EOP of the patient's hand (ξ_p), the technique injects damping to compensate for the difference. Consequently, using the proposed technique, the EOP of the patient's hand quantitatively defines the customized damping factor to modify the therapy (contrary to conventional conservative prefixed force caps in rehabilitation systems). To calculate $\eta_{min}(t)$, estimates of ξ_p and $\hat{\delta}_{th}$ are essential.

B. EOP Estimator for the Patient's Hand Reaction Dynamics

Considering the stability condition (14), the energy injected by the therapy terminal $\int_0^t f_P(\tau)^T\cdot v_p(\tau)\,d\tau$ during therapy delivery is measurable. This makes it possible to observe $\hat{\delta}_{th}$ in (23) under some conditions. However, there is no direct way to observe the passivity of the reaction dynamics of the patient's hand, i.e., $\int_0^t f_{react}(\tau)^T\cdot v_p(\tau)\,d\tau$. The aforementioned issue arises since $f_{react}(t)$ is not measurable during therapy and separating it from the exogenous force $f_p^*(t)$ in (2) is not possible. As a result, during rehabilitation, it is not possible to directly calculate ξ_p. In this paper, an identification scheme is proposed to estimate a lower bound for ξ_p for each user that can then be used in the control architecture (23), as an estimate for ξ_p.

Identification Procedure: To estimate ξ_p, an off-line identification scheme is proposed. Before the start of the therapy session, the patient is asked to allow the robot to perturb their hand while holding the robot's handle in a relaxed condition (with minimum grasp pressure). The robot provides movements of different frequencies/trajectories. The user's hand is perturbed for 60 seconds, using a stimulation trajectory that is a summation of ten sinusoids, in the range $0-3Hz$ in two degrees of freedom with a maximum amplitude of 1.5 cm. Since during off-line identification the patient does not apply exogenous forces, we have $f_p^*=0$ for the patient-robot interaction (2). Consequently, during the identification procedure, $\int_0^t f_{react}(\tau)\cdot v_P(\tau)^T\,d\tau = \int_0^t f_p(\tau)\cdot v_P(\tau)^T\,d\tau$ while both $f_p(t)$ and $v_p(t)$ are measurable. As a result, based on the considered passivity model (17) and using the collected data from the identification procedure, an estimate of the EOP for the patient's hand in relaxed condition can be calculated as

$$\xi_{p-relax} = \xi_p^* \quad \text{where} \quad \xi_p^* \leq \frac{\int_0^{T_e} f_{react}(\tau)\cdot v_P(\tau)^T\,d\tau}{\int_0^{T_e} v_p^T(\tau)\cdot v_P(\tau)^T\,d\tau} \quad (25)$$

In (25), $\xi_{p-relax}$ is the estimated EOP in the relaxed condition and $T_e = 60s$ is the duration of identification process.

Remark III. In this paper, the definition of a relaxed condition for the hand is when the grasp pressure is between

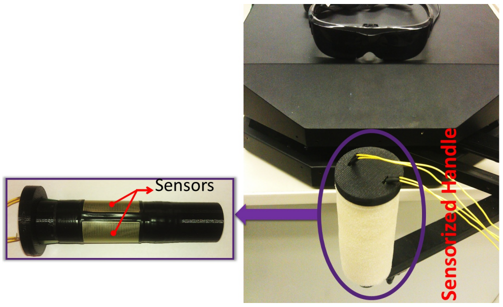

Fig. 4. The sensorized handle connected to the rehabilitation device

$2\% - 5\%$ of the maximum possible pressure. In order to measure the grasp pressure, a sensorized handle was constructed and connected to the rehabilitation robot as shown in Fig. 4. We observed that higher grasp pressure increases ξ_p. The aforementioned observation was tested for the current study on one healthy subject under an ethics approval from the University of Alberta's Research Ethics Board. For this purpose, both $\xi_{p-relax}$ and $\xi_{p-rigid}$ (EOP when grasp pressure is within $75\% - 85\%$ of the maximum possible value) are estimated. It is observed that increasing the grasp pressure increases the EOP to more than 400% of the relaxed condition (from 5.56 $N.s/m$ for $\xi_{p-relax}$ to 25.06 $N.s/m$ for $\xi_{p-rigid}$). Consequently, $\xi_{p-relax}$ is utilized in (23) as the lower-bound for ξ_p to ensure stability for different grasp pressures during various rehabilitation tasks. Once the lower bound of ξ_p is calculated ($i.e.$, $\xi_{p-relax}$), it is used as the estimate of the minimum EOP of the patient's hand and is defined by ξ_p^* in the proposed control scheme (23) to ensure system stability.

C. SOP Observer for the Therapy Terminal

In order to quantify ψ in (23), it is also required to calculate the SOP of the therapy terminal in real-time. Since $f_p(t)$ and $v_p(t)$ can be measured during rehabilitation tasks, the SOP of the therapy terminal can be observed through an energy observer, which takes $f_p(t) \cdot v_p(t)$ as the input power in real-time. To use the most recent data and to reduce the conservativeness of the system, forgetting factors are considered in calculating the passivity integrals. Assuming that the therapist does not change z_{th} frequently, the following regression model is utilized in an online recursive least-squares technique to find the estimate of $\hat{\delta}_{th}$ (i.e. $\hat{\delta}_{th}^*$):

$$\begin{aligned} Y_{th}(t) &= \Theta_{th}^T \Phi_{th}(t) \\ \text{when: } \Theta_{th} &= \hat{\delta}_{th}^*,\ \Phi_t h(t) = \int_0^t v_p^T(\tau) \cdot v_P(\tau)^T \, d\tau, \\ \text{and } \ Y_{th}(t) &= \int_0^t f_p(\tau) \cdot v_P(\tau)^T \, d\tau. \end{aligned} \quad (26)$$

After finding values for ξ_p and $\hat{\delta}_{th}$, the required damping can be calculated based on (23), where ξ_r is considered to address any estimation/identification error:

$$\eta(t) = \xi_r - \xi_p^* - \hat{\delta}_{th}^* \quad (27)$$

A schematic of the designed interaction including the stabilizer, SOP observer, and EOP estimator is shown in Fig. 5.

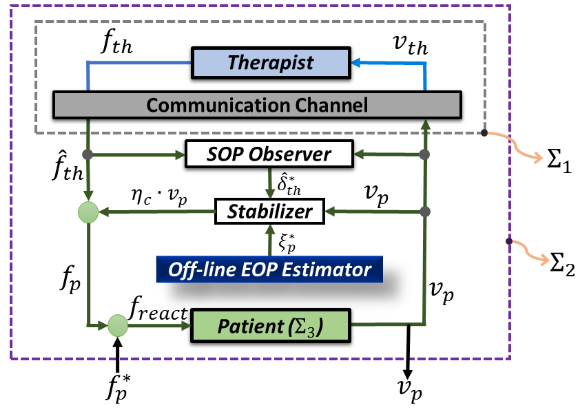

Fig. 5. The complete architecture of the proposed system.

V. EXPERIMENTAL RESULTS

Experimental results are provided to support the theory. The implemented system consists of the following:
(A) The master haptic device at the patient side is a 2-DOF planar upper-limb rehabilitation robot from Quanser Inc., that moves in the horizontal (X-Y) plane allowing for arm flexion-extension. The robot is shown in Figs. 1 and 4.
(B) The slave haptic device is a 6-DOF Quanser HD^2 haptic device locked in 4 degrees of freedom to provide a similar workspace to that of the master device.
(C) The virtual Environment (VE): is show in Fig. 2 for the implemented HTR system. A head-mounted visor (Fig. 1) is used on the patient's side to display the VE.

A. Passive and Active Therapy

In the first set of experiments, the operator, mimicking the role of the patient, tries to track the green target in the virtual reality display (shown in Fig. 2). The second operator who plays the role of the therapist initially applies resistive forces (phase I), to provide a passive environment, then applies assistive forces (phase II), to provide a non-passive environment. During the second phase, a round-trip time-varying communication delay of 80 $+20 \cdot Sin(12\pi t)$ ms is also introduced while in the first phase the communication delay is considered zero. As a result, the first phase represents the passive therapy phase and the second phase, which involves two sources of non-passivity, represents the active therapy phase. The goal is to evaluate the performance of the proposed scheme in addressing passive and active therapies.

The possible locations for the target are corners of the VE and one home position at the centre. The target location switches in a pseudo-random way to make a a star-shaped therapy trajectory. Both phases consist of 50 iterations of tracking. The tracking results are shown in Fig. 6.

As can be seen, the generated velocities and motion amplitudes for the case of assistive therapy are considerably higher than for the resistive therapy which means that the system was capable of properly delivering both types of actions through the non-passive interconnection and in a stable manner. In other words, the stabilizing scheme allows the therapist to provide assistance in the presence of the non-passivity of the interaction.

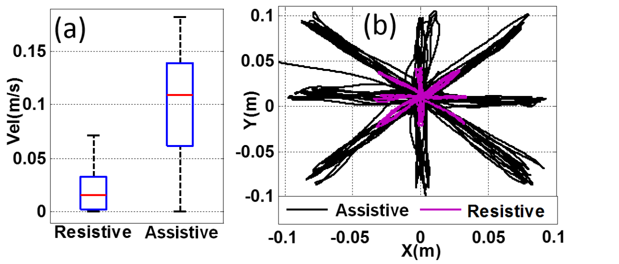

Fig. 6. Comparison between resistive therapy and delayed assistive therapy. (a) velocity distribution, and (b) position trajectories

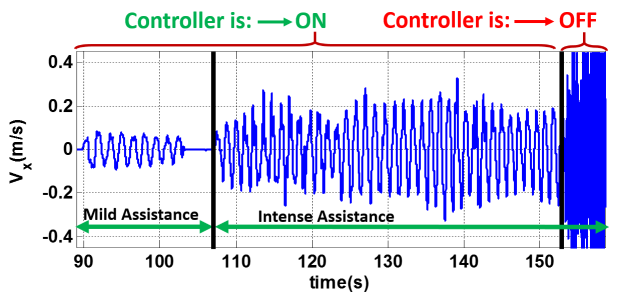

Fig. 7. Velocity trajectory for mild vs. intense therapy in the presence/absence of the proposed controller

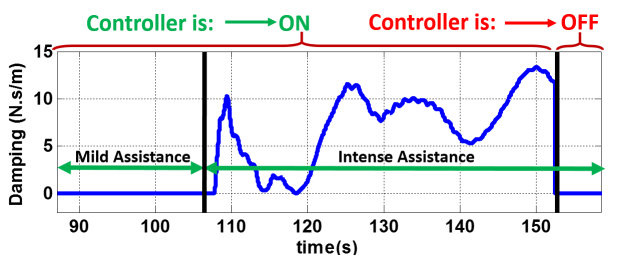

Fig. 8. Stabilizing damping calculated by the controller

B. Stability Evaluation

In the second set of experiments, the stability of the system was analyzed for a sinusoidal trajectory. The round-trip delay is $80 + 20 \cdot Sin(12\pi t)$ ms. First, the therapist provides mild assistance at $t = 87s$ when the controller ensures that the damping is zero. As a result, no modification is delivered. Then, the therapist starts the intense assistance at $t = 107s$ at which time the controller starts injecting damping to modify the received force to deal with the potential instability while letting the therapist provide assistance through the delayed HTR system. At $t = 152s$, the controller is turned off while the therapist still provides intense assistance. This results in system instability (high-frequency high-amplitude force/velocity oscillations) which highlights the effectiveness of the proposed stabilizing scheme. The velocity trajectory in the X direction and the damping injected by the scheme are given in Fig. 7 and Fig. 8. Also the force modulation for mild and intense assistance are given in Fig. 9 and Fig. 10.

Our ongoing work focuses on developing a statistical map between the grasp pressure and the EOP of the upper-limb and utilizing real-time measurements of the grasp pressure to estimate ξ_p and adaptively tune the control gains.

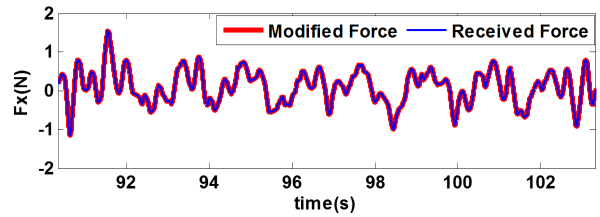

Fig. 9. Force modulation: mild assistance

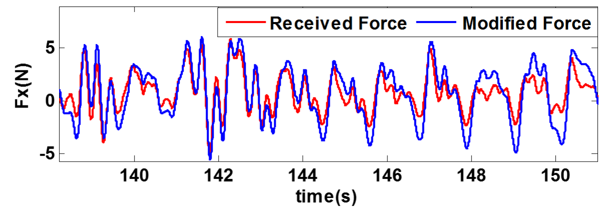

Fig. 10. Force modulation: intense assistance

REFERENCES

[1] H. I. Krebs and N. Hogan, "Therapeutic robotics: A technology push," *Proceedings of the IEEE*, vol. 94, no. 9, pp. 1727–1738, 2006.

[2] N. Hogan, *et al.*, "Motions or muscles? some behavioral factors underlying robotic assistance of motor recovery," *Journal of rehab research and development*, vol. 43, no. 5, pp. 605–618, 2006.

[3] *http://interactive-motion.com/healthcarereform/technology/.*

[4] O. Barzilay and A. Wolf, "Adaptive rehabilitation games," *J. of Electromyography and Kinesiology*, vol. 23, no. 1, pp. 182 – 189, 2013.

[5] S. F. Atashzar, *et al.*, "Networked teleoperation with non-passive environment: Application to tele-rehabilitation," in *IEEE/RSJ Int. Conf. on Intelligent Robots and Systems*, 2012, pp. 5125–5130.

[6] S. F. Atashzar, *et al.*, "Projection-based force reflection algorithms for teleoperated rehabilitation therapy," in *IEEE/RSJ International Conference on Intelligent Robots and Systems*, 2013, pp. 477–482.

[7] R. Tao and M. Tavakol, "Haptic teleoperation based rehabilitation systems for task-oriented therapy," *MSc thesis*, 2014.

[8] A. Butler, *et al.*, "Expanding tele-rehabilitation of stroke through in-home robot-assisted therapy," *Int J Phys Med Rehabil*, vol. 2, no. 184, p. 2, 2014.

[9] H. Kim, *et al.*, "Kinematic data analysis for post-stroke patients following bilateral versus unilateral rehabilitation with an upper limb wearable robotic system," *IEEE Trans. on Neural Systems and Rehabilitation Engineering*, vol. 21, no. 2, pp. 153–164, 2013.

[10] S. F. Atashzar, *et al.*, "Control of time-delayed telerobotic systems with flexible-link slave manipulators," in *IEEE/RSJ International Conference on Intelligent Robots and Systems*. IEEE, 2012.

[11] K. Hashtrudi-Zaad and S. E. Salcudean, "Analysis of control architectures for teleoperation systems with impedance/admittance master and slave manipulators," *The International Journal of Robotics Research*, vol. 20, no. 6, pp. 419–445, 2001.

[12] K. Hashtrudi-Zaad and S. Salcudean, "Transparency in time-delayed systems and the effect of local force feedback for transparent teleoperation," *IEEE Tran. on Robotics and Automation*, vol. 18, no. 1, pp. 108–114, 2002.

[13] S. F. Atashzar, *et al.*, "Involuntary movement during haptics-enabled robotic rehabilitation: Analysis and control design," in *IEEE/RSJ Int. Conf. on Intelligent Robots and Systems*, 2014, pp. 3561–3566.

[14] E. Nuno, *et al.*, "A globally stable pd controller for bilateral teleoperators," *IEEE Tran. on Robotics*, vol. 24, no. 3, pp. 753–758, 2008.

[15] M. Vidyasagar, *Nonlinear systems analysis*. SIAM, 2002, vol. 42.

[16] A. Aziminejad, *et al.*, "Transparent time-delayed bilateral teleoperation using wave variables," *IEEE Transactions on Control Systems Technology*, vol. 16, no. 3, pp. 548–555, 2008.

[17] J. Forbes and C. Damaren, "Passive linear time-varying systems: State-space realizations, stability in feedback, and controller synthesis," in *American Control Conference*, June 2010, pp. 1097–1104.

[18] A. Jazayeri, *et al.*, "Stability analysis of teleoperation systems under strictly passive and non-passive operator," in *World Haptics Conference*, April 2013, pp. 695–700.

[19] D. J. Hill and P. J. Moylan, "Stability results for nonlinear feedback systems," *Automatica*, vol. 13, no. 4, pp. 377–382, 1977.

[20] H. K. Khalil and J. Grizzle, *Nonlinear systems*. Prentice hall, Upper Saddle River, 2002, vol. 3.